arXiv:1207.4890v2 [hep-ph] 2 Aug 2012

Phase diagrams in nonlocal PNJL models constrained by Lattice QCD results

G. A. Contrera[1,2,5], A. G. Grunfeld[2,3,4], D. B. Blaschke [5,6]

[1] *Gravitation, Astrophysics and Cosmology Group, FCAyG, UNLP, La Plata, Argentina*

[2] *CONICET, Rivadavia 1917, 1033 Buenos Aires, Argentina*

[3] *Department of Physics, Sultan Qaboos University,*
P.O.Box: 36 Al-Khode 123 Muscat, Sultanate of Oman

[4] *Departamento de Física, Comisión Nacional de*
Energía Atómica, (1429) Buenos Aires, Argentina

[5] *Institute for Theoretical Physics, University of Wrocław, 50-204 Wrocław, Poland*

[6] *Bogoliubov Laboratory for Theoretical Physics, JINR Dubna, 141980 Dubna, Russia*

(Dated: August 3, 2012)

We discuss a scheme for extracting the location of the critical endpoint in the QCD phase diagram based on nonlocal PNJL models including vector interactions. The formfactors of the covariant model are constrained by lattice QCD data for the quark propagator. The strength of the vector coupling is adjusted such as to reproduce the slope of the pseudocritical temperature of the chiral phase transition at low chemical potential extracted recently from lattice QCD simulations. Our study supports the existence of a critical endpoint in the QCD phase diagram. For the more favorable nonlocal model, with wave function renormalization (set B and set C), the critical endpoint is located as $(T_{\rm CEP}, \mu_{\rm CEP}) = (129.8 \text{ MeV}, 276.6 \text{ MeV})$ and $(T_{\rm CEP}, \mu_{\rm CEP}) = (69.9 \text{ MeV}, 319.1 \text{ MeV})$ for set B and set C, respectively.

The conjecture for the existence of a critical endpoint (CEP) of first order phase transitions in the QCD phase diagram is the basis for recent as well as future beam energy scan (BES) programs in relativistic heavy-ion collision experiments at RHIC, SPS, NICA and FAIR which try to identify the parameters of its position $(T_{\rm CEP}, \mu_{\rm CEP})$. The theoretical situation is very unsatisfactory since the predictions for this position form merely a skymap in the $T - \mu$ plane [1].

The now well-established results from lattice QCD that at zero and small chemical potential μ, predict coincident chiral and deconfinement crossover transitions at a pseudocritical temperature of $T_c(0) = 154 \pm 9$ MeV for 2+1 flavours [2] and a value of $T_c(0) \sim 170$ MeV for two flavours [3]. Then, the underlying idea is to use effective theories based on QCD, which reproduce lattice results at vanishing μ, and see whether the predictions can be extrapolated at high chemical potential. That leaves us with a variety of possibilities for the phase structure at non zero μ, among them we want to mention the following ones

- no CEP at all [4], since the transition is crossover in the whole phase diagram,
- no CEP, but a Lifshitz point [5],
- one CEP, but with largely differing predictions of its position [1],
- second CEP [6–8],
- CEP and triple point, possibly coincident, due to another phase (i.e. colour superconducting [9] or quarkyonic [10] matter) at low temperatures and high densities.

This situation is rather unsatisfactory in view of the upcoming experimental programmes. In the present work we discuss the existence and location of a CEP within the frame of nonlocal chiral quark models coupled to the Polyakov loop potential on the selfconsistent meanfield level.

The Lagrangian for the $SU(2)_f$ non local models, including vector channel interactions, is given by

$$\mathcal{L} = \bar{q}(i\not{D} - m_0)q + \mathcal{L}_{\text{int}} + \mathcal{U}(\Phi) \ , \tag{1}$$

where q is the $N_f = 2$ fermion doublet $q \equiv (u, d)^T$, and m_0 is the current quark mass (we consider isospin symmetry, that is $m_0 = m_u = m_d$). The covariant derivative is defined as $D_\mu \equiv \partial_\mu - iA_\mu$, where A_μ are colour gauge fields.

The nonlocal interaction channels are given by

$$\mathcal{L}_{\text{int}} = -\frac{G_S}{2}\Big[j_a(x)j_a(x) - j_P(x)j_P(x)\Big] - \frac{G_V}{2} j_V(x)\, j_V(x), \tag{2}$$

where the nonlocal currents are

$$\begin{aligned} j_a(x) &= \int d^4z\ g(z)\ \bar{q}\left(x+\frac{z}{2}\right)\ \Gamma_a\ q\left(x-\frac{z}{2}\right)\ , \\ j_P(x) &= \int d^4z\ f(z)\ \bar{q}\left(x+\frac{z}{2}\right)\ \frac{i\overleftrightarrow{\not\partial}}{2\ \kappa_p}\ q\left(x-\frac{z}{2}\right)\ , \\ j_V(x) &= \int d^4z\ g(z)\ \bar{q}\left(x+\frac{z}{2}\right)\ \gamma^0\ q\left(x-\frac{z}{2}\right) \end{aligned} \tag{3}$$

with $\Gamma_a = (\Gamma_S, \Gamma_P) = (\mathbb{1}, i\gamma_5\vec{\tau})$ for scalar and pseudoscalar currents respectively, and $u(x')\overleftrightarrow{\partial}v(x) = u(x')\partial_x v(x) - \partial_{x'}u(x')v(x)$. The functions $g(z)$ and $f(z)$ in (3) are nonlocal covariant form factors characterizing the corresponding interactions. The scalar-isoscalar component of the $j_a(x)$ current will generate the momentum dependent quark mass in the quark propagator, while the "momentum" current, $j_P(x)$, will be responsible for a momentum dependent wave function renormalization (WFR) of this propagator. Note that the relative strength between both interaction terms is controlled by the mass parameter κ_p introduced in (3). Finally, $j_V(x)$ represents the vector channel interaction current, whose coupling constant G_V is usually taken as a free parameter.

In what follows it is convenient to Fourier transform into momentum space. Since we are interested in studying the characteristics of the chiral phase transition we have to extend the effective action to finite temperature T and quark chemical potential μ [33]. In the present work this is performed by using the Matsubara and imaginary time formalisms. Concerning the gluon fields we use the same prescription as in previous works [11, 12], but in our present case we have chosen a μ-dependent logarithmic effective potential described in [13].

$$\mathcal{U}(\Phi, T, \mu) = (a_0T^4 + a_1\mu^4 + a_2T^2\mu^2)\Phi^2 + a_3T_0^4\ln(1 - 6\Phi^2 + 8\Phi^3 - 3\Phi^4), \tag{4}$$

where $a_0 = -1.85$, $a_1 = -1.44\text{x}10^{-3}$, $a_2 = -0.08$, $a_3 = -0.40$. In the present work we set the T_0 parameter by using the value corresponding to two flavours $T_0 = 208$ MeV, as it has been suggested in [14], and used in subsequent approachs, including the nonlocal PNJL [15] and Polyakov loop-DSE models [16].

Finally, to fully specify the nonlocal models under consideration we fix the model parameters as well as the form factors $g(q)$ and $f(q)$ following [12, 17], i.e. considering two different types of functional dependencies for these form factors: exponential forms (set A and set B) and Lorentzians (Set C). In order to compare with some recent results [4], we have included a local form factor, using for this case the parameters in [18].

The model inputs can be constrained with recent results from lattice QCD studies. In particular, the form factors of the nonlocal interaction [17] have been chosen such as to reproduce the dynamical mass function $M(p)$ and the WFR $Z(p)$ of the quark propagator in the vacuum [19]. In Figure 1 we show the shapes of normalized dynamical masses and WFR for the models under discussion here, i.e., the nonlocal models of set A (rank-one), set B and set C (rank-two) as well as the local limit. This figure generalizes the corresponding Figure 1 in [17], by including the local limit case and showing the line $Z(p) = 1$ for both, set A and the local case. It is easy to recognize the better agreement between the lattice results and the more complete model, namely nonlocal PNJL with WFR, in its two form factor parametrizations given by set B and set C.

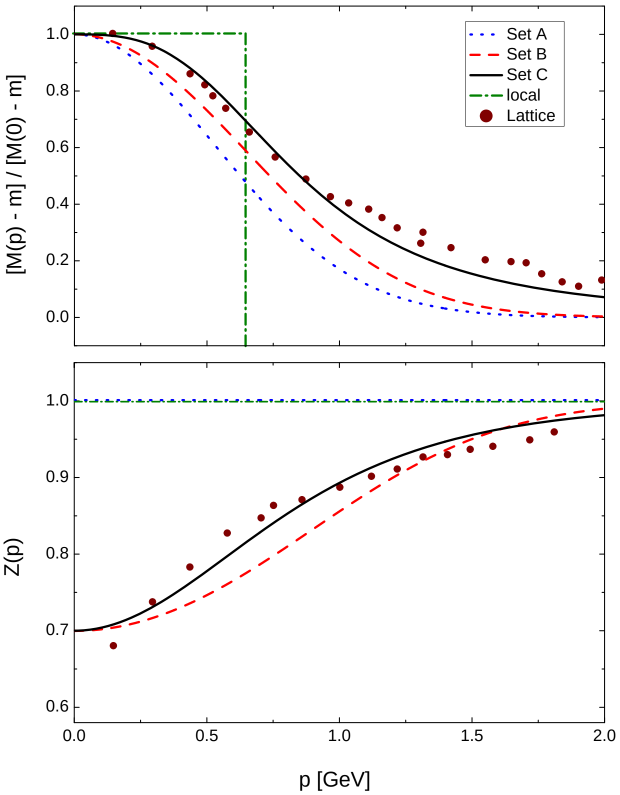

FIG. 1: Normalized dynamical masses and wave function renormalization for the different form factors under study, fitted to lattice data [19], extended from [17] by inclusion of local model [18].

Within this framework the mean field thermodynamical potential $\Omega^{\rm MFA}$ results

$$\begin{aligned}\Omega^{\rm MFA} = & -\ 4T \sum_c \sum_n \int \frac{d^3\vec{p}}{(2\pi)^3} \ln \left[\frac{(\tilde{\rho}^c_{n,\vec{p}})^2 + M^2(\rho^c_{n,\vec{p}})}{Z^2(\rho^c_{n,\vec{p}})} \right] \\ & + \frac{\sigma_1^2 + \kappa_p^2\ \sigma_2^2}{2\,G_S} - \frac{\omega^2}{2G_V}\ + \mathcal{U}(\Phi, T). \qquad (5)\end{aligned}$$

where $M(p)$ and $Z(p)$ are given by

$$\begin{aligned} M(p) &= Z(p)\,[m + \sigma_1\ g(p)]\,, \\ Z(p) &= [1 - \sigma_2\ f(p)]^{-1}\,. \qquad (6)\end{aligned}$$

In addition, as in [12] we have considered

$$\left(\rho^c_{n,\vec{p}}\right)^2 = \Big[(2n+1)\pi T - i\mu + \phi_c\Big]^2 + \vec{p}^{\,2}\ , \qquad (7)$$

where the quantities ϕ_c are given by the relation $\phi = \mathrm{diag}(\phi_r, \phi_g, \phi_b)$. Namely, $\phi_c = c\ \phi_3$ with $c = 1, -1, 0$ for r, g, b, respectively. In the case of $\left(\tilde{\rho}^c_{n,\vec{p}}\right)$ we have used the same definition as in (7) but shifting the chemical potential according to

$$\tilde{\mu} = \mu\ - \omega\ g(p)\ Z(p). \qquad (8)$$

The $\Omega^{\rm MFA}$ turns out to be divergent and, thus, needs to be regularized. For this purpose we use the same prescription as in [12, 20]. The mean field values $\sigma_{1,2}$, ω and ϕ_3 at a given temperature or chemical potential, are obtained from a set of four coupled "gap" equations which come from the minimization of the regularized thermodynamical potential, that is

$$\frac{\partial \Omega^{\rm MFA}_{reg}}{\partial \sigma_1} = \frac{\partial \Omega^{\rm MFA}_{reg}}{\partial \sigma_2} = \frac{\partial \Omega^{\rm MFA}_{reg}}{\partial \omega} = \frac{\partial \Omega^{\rm MFA}_{reg}}{\partial \phi_3} = 0. \qquad (9)$$

We also want to include in our analysis the results arising from a local PNJL model. For that purpose, we started from the Lagrangian in [21] with two flavours instead of three. Moreover, we consider that the chemical potential is shifted by

$$\tilde{\mu} = \mu\ - \omega. \qquad (10)$$

We use the same set of parameters as in [18].

The vector coupling constant G_V is considered a free parameter which in the mean field approximation (MFA) may be adjusted such as to reproduce the behaviour of $T_c(\mu)$ which has recently been obtained by Taylor expansion technique in lattice QCD [22]

$$T_c(\mu)/T_c(0) = 1 - \kappa(\mu/T_c)^2 + \mathcal{O}[(\mu/T_c)^4], \qquad (11)$$

with $\kappa = 0.059(2)(4)$ being the curvature.

Note that this result is not yet based on continuum extrapolated lattice results, so that discretization errors has to be expected. However, we are interested to present here a scheme for constraining effective QCD models. The quality of predictions can subsequently be improved by using better lattice QCD data and constant discretization schemes.

To determine the curvatures we plotted the pseudocritical temperatures of the crossover transitions at low values of μ/T for different ratios $\eta_V = G_V/G_S$. An example of this is shown in Figure 2 for set C (the corresponding plots for the other models are qualitatively very similar). The fit of the lattice QCD results (11) is also shown. The grey zone corresponds to the error in the coefficient κ obtained in [22].

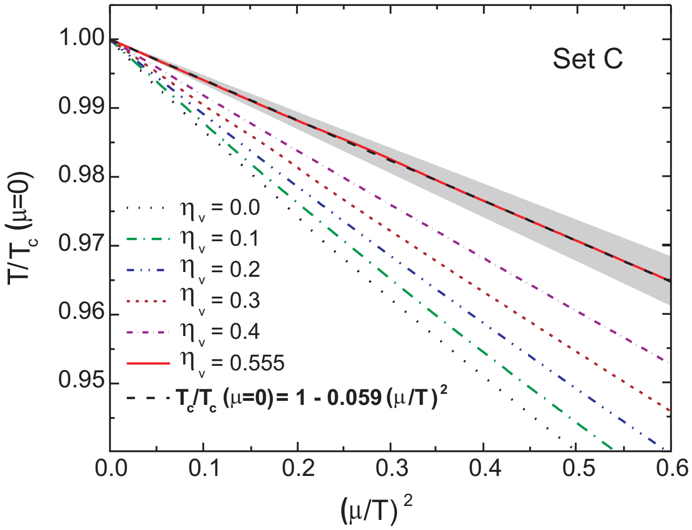

FIG. 2: Chiral crossover transitions at low values of μ/T for different values of strengths of the vector coupling $\eta_V = G_V/G_S$ for Set C. The dashed line corresponds to the lattice QCD prediction of $\kappa = 0.059(2)(4)$ [22].

In Figure 3 we compare the lattice result with the values for the coefficient κ obtained within the nonlocal PNJL models and the local one. There, the horizontal line corresponds to the lattice QCD prediction of $\kappa = 0.059(2)(4)$ [22] and the grey zone represents its error. Note that for the more complete model (set B and set C) the curvatures are closer to each other than in the case of set A and local ones.

We would like to remark that while the analysis of κ has been performed for $N_f = 2+1$ simulations, the chemical potential μ concerns only the two light flavours. Therefore, our extraction of κ from the nonlocal PNJL models for the 2-flavour case may be in order.

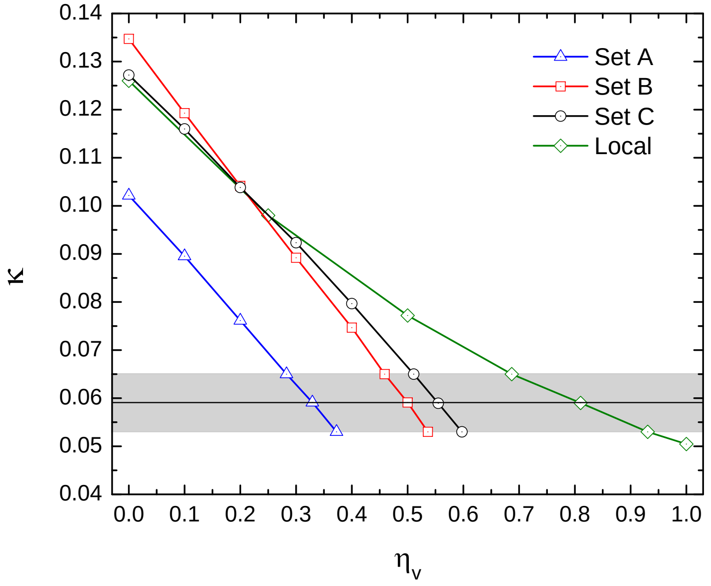

FIG. 3: Curvature κ of the pseudocritical temperature $T_c(\mu)$ of the chiral crossover transition at low values of μ/T. The horizontal line corresponds to the lattice QCD prediction of $\kappa = 0.059(2)(4)$ [22].

In Figure 4 we compare the two different classes of nonlocal models discussed in this work. The nonlocal model for set B and set C cases, contains WFR and dynamical (running) quark mass effects and thus is closer to full QCD. Therefore, we suggest that statements about the existence and location of the CEP within set A and the local model should be less trustworthy than those of set B and set C.

In Figure 4 we have also shown a grey zone corresponding to the range of η_V values obtained by taking into account the error in the lattice determination of κ [22]. The error bars in the CEP's indicate the distances to the CEP positions for the corresponding η_V values that fit the error limits. Note that in the local model, for fitting the lattice QCD value a larger vector coupling is required than in the nonlocal ones. The consequences for predictions about the existence and location of the CEP are dramatic, see Figure 5. On the other hand, we found that using the Polyakov loop potential (4) from [13], a crossover region and a CEP can be obtained for set A, even for $T_0 = 208$ MeV, contrarily to what has been reported in [15, 16], where the Polyakov loop potential from [23] has been used [34].

The results summarized in Figure 5 indicate that the absolute value of the critical tem-

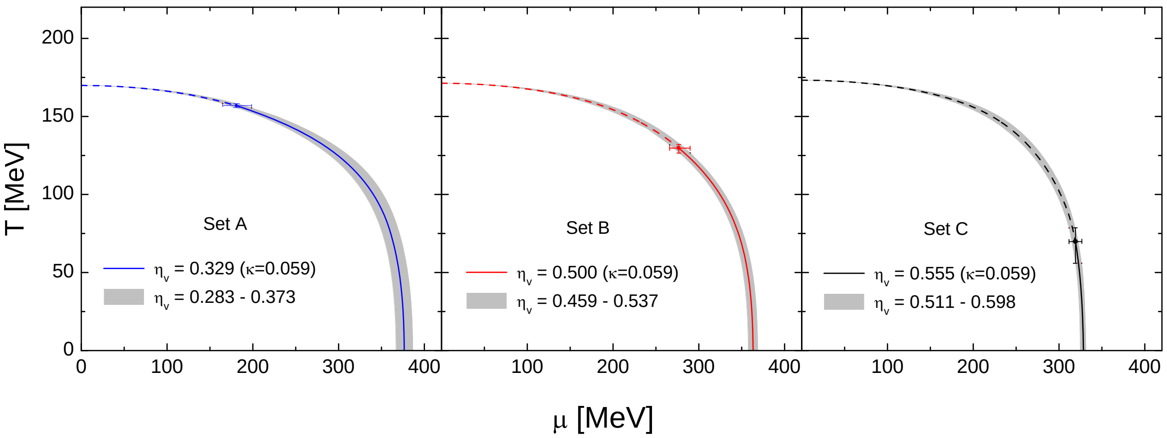

FIG. 4: Phase diagrams for the non local models for the values of η_V that best fit the lattice QCD results in [22].

perature $T_c(0)$ of nonlocal covariant PNJL models is rather insensitive to the choice of the form factors parametrizing the momentum dependence of dynamical (running) mass function and WFR of the quark propagator as measured on the lattice at zero temperature [19], whereas the position of the CEP and critical chemical potential at $T = 0$ strongly depends on it. Nevertheless, the value of $T_c(0)$ in the local model is significantly different (larger) than in the nonlocal ones.

The region of CEP's suggested by our study is between the results for set B and set C, i.e. $(T_{\rm CEP}, \mu_{\rm CEP}) = (129.8\ {\rm MeV}, 276.6\ {\rm MeV})$ and $(69.9\ {\rm MeV}, 319.1\ {\rm MeV})$, respectively.

This means that the search for CEP signatures in the BES programs is justified and should be continued. The energy range of the NICA and FAIR facilities shall be particularly promising. As a characteristic feature of the region around the CEP any phase transition signals based on changes in the bulk properties are not pronounced. Therefore, sensible observables are required for the identification of the CEP position like, e.g., higher moments of the identified particle distributions [24, 25] or the flow of nuclear clusters [26].

In conclusion, we have presented progress in the extraction of the CEP location in the QCD phase diagram based on nonlocal PNJL models constrained by lattice QCD. Note that in this exploratory study the lattice QCD data for the quark propagator data and for the curvature of the pseudocritical line are obtained with different lattice actions. A more consistent study should be based on the same discretization of the action, provide a continuum extrapolation and work with physical quark masses.

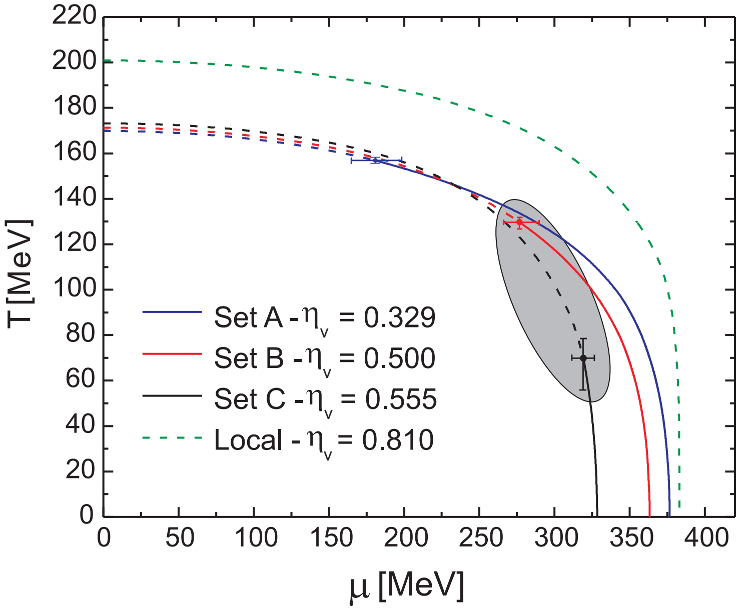

FIG. 5: (Colour online) Phase diagrams with (pseudo)critical temperatures $T_c(\mu)$ and critical points for nonlocal PNJL models (set A-C) compared to the local one. Dashed (full) lines correspond to crossover (first order) transitions. The vector coupling strength η_V is chosen so that these models reproduce the lattice QCD result $\kappa = 0.059(2)(4)$ [22] for the curvature at low μ-values. The corresponding values for $T_c(\mu = 0)$ (in MeV) are 169.9, 171.3, 173.2 and 200.9, for Sets A, B, C and local, respectively. The highlighted region denotes the CEP position favored by the present study.

As a next step it is necessary to investigate the robustness of the results of the nonlocal PNJL models when modifying the choice of the Polyakov-loop potential taking into account recent developments [27–29] and, in particular, when going beyond the mean field approximation. A scheme for going beyond the meanfield in nonlocal PNJL models by including hadronic correlations (bound states and their dissociation in the continuum of scattering states) has recently been developed [30] and shall be generalized for studies of the chiral and deconfinement phase transition in the QCD phase diagram. A key quantity for such studies will be the hadronic spectral function and first results using a generic ansatz [31] for joining the hadron resonance gas and PNJL approaches are promising [32].

Acknowledgements

We would like to thanks to C. Schmidt, K. Redlich, N. Scoccola and K. Rajagopal for useful comments and discussions. D.B. acknowledges hospitality and support during his visit at University of Bielefeld and funding of his research provided by the Polish NCN under the "Maestro" Grant programme as well as by the Russian Fund for Basic Research under Grant No. 11-02-01538-a. G.C. is grateful for support by CONICET (Argentina) and by the Polish Ministry for Science and Higher Education within the CompStar-POL project.

---

[1] M. A. Stephanov, PoS LAT **2006**, 024 (2006).

[2] A. Bazavov, T. Bhattacharya, M. Cheng, C. DeTar, H. T. Ding, S. Gottlieb, R. Gupta and P. Hegde *et al.*, Phys. Rev. D **85**, 054503 (2012).

[3] S. Ejiri, Nucl. Phys. Proc. Suppl. **94**, 19 (2001)

[4] N. M. Bratovic, T. Hatsuda and W. Weise, arXiv:1204.3788 [hep-ph].

[5] S. Carignano, D. Nickel, and M. Buballa, Phys. Rev. D **82**, 054009 (2010).

[6] M. Kitazawa, T. Koide, T. Kunihiro and Y. Nemoto, Prog. Theor. Phys. **108**, 929 (2002).

[7] D. Blaschke, M. K. Volkov and V. L. Yudichev, Eur. Phys. J. A **17**, 103 (2003).

[8] T. Hatsuda, M. Tachibana, N. Yamamoto and G. Baym, Phys. Rev. Lett. **97**, 122001 (2006).

[9] D. Blaschke, H. Grigorian, A. Khalatyan and D. N. Voskresensky, Nucl. Phys. Proc. Suppl. **141**, 137 (2005).

[10] A. Andronic, D. Blaschke, P. Braun-Munzinger, J. Cleymans, K. Fukushima, L. D. McLerran, H. Oeschler and R. D. Pisarski *et al.*, Nucl. Phys. A **837**, 65 (2010).

[11] G. A. Contrera, D. Gomez Dumm and N. N. Scoccola, Phys. Lett. B **661** (2008) 113.

[12] G. A. Contrera, M. Orsaria and N. N. Scoccola, Phys. Rev. D **82**, 054026 (2010).

[13] V. A. Dexheimer and S. Schramm, Phys. Rev. C **81**, 045201 (2010).

[14] B. -J. Schaefer, J. M. Pawlowski and J. Wambach, Phys. Rev. D **76**, 074023 (2007).

[15] V. Pagura, D. Gómez Dumm and N. N. Scoccola, Phys. Lett. B **707**, 76 (2012).

[16] D. Horvatic, D. Blaschke, D. Klabucar, O. Kaczmarek, Phys. Rev. D **84**, 016005 (2011).

[17] S. Noguera and N. N. Scoccola, Phys. Rev. D **78**, 114002 (2008).

[18] D. Gomez Dumm, D. B. Blaschke, A. G. Grunfeld and N. N. Scoccola, Phys. Rev. D **78**,

114021 (2008).

[19] M. B. Parappilly, P. O. Bowman, U. M. Heller, D. B. Leinweber, A. G. Williams and J. B. Zhang, Phys. Rev. D **73**, 054504 (2006).

[20] D. Gomez Dumm and N. N. Scoccola, Phys. Rev. C **72**, 014909 (2005).

[21] K. Fukushima, Phys. Rev. D **77**, 114028 (2008).

[22] O. Kaczmarek, F. Karsch, E. Laermann, C. Miao, S. Mukherjee, P. Petreczky, C. Schmidt, W. Soeldner and W. Unger, Phys. Rev. D **83**, 014504 (2011).

[23] S. Roessner, C. Ratti and W. Weise, Phys. Rev. D **75**, 034007 (2007).

[24] B. Friman, F. Karsch, K. Redlich and V. Skokov, Eur. Phys. J. C **71**, 1694 (2011).

[25] F. Karsch and C. Schmidt, *NICA White Paper* **v7.02**, 104 (2012).

[26] P. Danielewicz, T. Klähn, W. Reisdorf and D. Blaschke, *NICA White Paper* **v7.02**, 117 (2012).

[27] C. Sasaki and K. Redlich, arXiv:1204.4330 [hep-ph].

[28] M. Ruggieri, P. Alba, P. Castorina, S. Plumari, C. Ratti and V. Greco, arXiv:1204.5995 [hep-ph].

[29] K. Fukushima and K. Kashiwa, arXiv:1206.0685 [hep-ph].

[30] A. E. Radzhabov, D. Blaschke, M. Buballa and M. K. Volkov, Phys. Rev. D **83**, 116004 (2011).

[31] D. B. Blaschke, J. Berdermann, J. Cleymans and K. Redlich, Phys. Part. Nucl. Lett. **8**, 811 (2011); Few Body Systems **53**, 99 (2012).

[32] L. Turko, D. Blaschke, D. Prorok and J. Berdermann, Acta Phys. Polon. Supp. **5**, 485 (2012).

[33] The corresponding values for baryon chemical potential μ_B can be easily obtained from the relation $\mu_B = 3\ \mu$.

[34] Note that in the low-μ region the differences in the chiral transition obtained with each effective potential are mainly due to the definition of the corresponding logarithmic term in the Polyakov loop potential.